Large-Scale Synthesis and Phase Transformation of CuSe, $CuInSe_2$, and $CuInSe_2/CuInS_2$ Core/Shell Nanowire Bundles

Jun Xu,[†] Chun-Sing Lee,[†,*] Yong-Bing Tang,[†] Xue Chen,[†] Zhen-Hua Chen,[†] Wen-Jun Zhang,[†] Shuit-Tong Lee,[†] Weixin Zhang,[‡,*] and Zeheng Yang[‡]

[†]Center of Super-Diamond and Advanced Films (COSDAF), and Department of Physics and Materials Science, City University of Hong Kong, Hong Kong SAR, People's Republic of China, and [‡]School of Chemical Engineering, Hefei University of Technology, Hefei, Anhui 230009, People's Republic of China

ABSTRACT Facile chemical approaches for the controllable synthesis of CuSe, $CuInSe_2$ nanowire, and $CuInSe_2/CuInS_2$ core/shell nanocable bundles were developed. Hexagonal CuSe nanowire bundles with lengths up to hundreds of micrometers, consisting of many aligned nanowires with a diameter of about 10−15 nm, were prepared by reacting cubic $Cu_{2-x}Se$ nanowire bundles with a sodium citrate solution at room temperature. The CuSe nanowire bundles were then used as self-sacrificial templates for making bundles of tetragonal chalcopyrite $CuInSe_2$ nanowires by reacting with $InCl_3$ *via* a solvothermal process. Furthermore, bundles of $CuInSe_2/CuInS_2$ core/shell nanocables were obtained by adding sulfur to the reaction system, and the shell thickness of the polycrystalline $CuInS_2$ in the nanocables increased with increasing S/Se molar ratios. It was found that the small radius of copper ions allows their fast outward diffusion from the interior to the surface of nanowires to react with sulfur atoms/anions and indium ions to form a $CuInS_2$ shell. Enhanced optical absorption in the vis−NIR region of $CuInSe_2/CuInS_2$ core/shell nanocable bundles is demonstrated, which is considered beneficial for applications in optoelectronic devices and solar energy conversion.

KEYWORDS: CuSe · $CuInSe_2$ · $CuInS_2$ · bundles · core/shell nanocables · phase transformation

Copper chalcogenides (CuSe, CuS) and their ternary ($CuInSe_2$, $CuGaSe_2$, $CuInS_2$) and quartenary compounds ($Cu(In_{1-x}Ga_x)Se_2$, $CuIn(Se_{1-x}S_x)_2$) have attracted much interest in recent years owing to their outstanding electro-optical properties.[1−6] Among them, the I−III−VI_2 chalcopyrite semiconductors are among the most promising light-absorbing materials for photovoltaic applications because of their suitable band gaps, high absorption coefficients, and good radiation stabilities.[7−9] Thin-film solar cells of $Cu(In_{1-x}Ga_x)Se_2$ have achieved record conversion efficiencies as high as 21.5%.[10] Chalcopyrite $CuInSe_2$, with a direct band gap of ~1.04 eV, has a high absorption coefficient over the UV−vis range, which is on the order of 10^5 cm^{-1} for the bulk and 10^4 cm^{-1} for thin films.[11,12] In order to achieve a better match to the solar spectrum, it is desirable to widen the band gap of $CuInSe_2$ by about 0.2−0.5 eV. This can typically be achieved *via* incorporation of Ga or S. The band gap of $CuInS_2$ (~1.53 eV) is well-matched to the solar spectrum for photovoltaic performance.[13] With such consideration, heterogeneous $CuInSe_2/CuInS_2$ core/shell nanostructures may be considered as a promising system for solar energy conversion applications.

While several approaches have been developed to fabricate $CuInSe_2$ thin films, including selenization of metal precursors,[14] electrodeposition,[15] hot wall deposition,[16] chemical vapor deposition,[17] magnetron sputtering,[18] paste coating,[19] *etc.*, methods for preparing $CuInSe_2$ nanostructures with controlled morphologies are so far limited. Up to now, there are only a few reports on the synthesis of $CuInSe_2$ nanocrystals using solvothermal methods,[20−25] VLS techniques,[26] and solid-state reactions.[27] For example, Qian's group[20,21] has synthesized $CuInSe_2$ nanoparticles, nanowhiskers, and nanorods *via* solvothermal reactions of Cu, In, and Ga salts/elements with selenium powders in ethylenediamine. Guo *et al.*[23] and Koo *et al.*[24] have prepared, respectively, $CuInSe_2$ nanorings with hexagonal shape and nanocrystals with trigonal pyramidal shape using oleylamine as solvent. Peng *et al.*[26] have reported the synthesis of In_2Se_3 and $CuInSe_2$ nanowires by VLS techniques. From a solid-state reaction between an In_2Se_3 nanowire and contacting copper pads, an individual $CuInSe_2$ nanowire has also been synthesized.[27] Nevertheless, to our best knowledge, there is so far no

*Address correspondence to apcslee@cityu.edu.hk, wxzhang@hfut.edu.cn.

Received for review October 5, 2009 and accepted March 03, 2010.

Published online March 8, 2010.
10.1021/nn9013627

report on a templating synthesis of $CuInSe_2$ nanostructures in large scale under relatively mild conditions. In this work, we develop a simple and effective method for chemically converting bundles of $Cu_{2-x}Se$ nanowires to bundles of CuSe and $CuInSe_2$ nanowires as well as bundles of $CuInSe_2/CuInS_2$ core/shell nanocables with different S/Se molar ratios.

RESULTS AND DISCUSSION

$Cu_{2-x}Se$ nanowire bundles with diameters of 200−400 nm and lengths up to hundreds of micrometers (see Supporting Information, Figure S1) have been prepared by a water-evaporation-induced self-assembly method.[28] Using the $Cu_{2-x}Se$ nanowire bundles as templates, CuSe nanowire bundles with the same morphologies were obtained by reaction with aqueous sodium citrate solution at room temperature. As an important biological ligand,[29] sodium citrate molecules, each with three carboxylate groups, can strongly chelate copper ions to form a stable complex of $[(C_6H_5O_7)Cu]^-$ due to its large formation constants ($K = 10^{14.2}$).[30] The chemical reaction may take place as follows

$$2Cu_{2-x}Se + (1-x)O_2 + 2(1-x)C_6H_5O_7^{3-} + 2(1-x)H_2O \rightarrow 2CuSe + 2(1-x)[(C_6H_5O_7)Cu]^- + 4(1-x)OH^-$$

Figure 1a shows a typical SEM image of the CuSe nanowire bundles with lengths up to hundreds of micrometers. A high-magnification SEM image in Figure 1b reveals that the bundles with diameters of 200−400 nm consist of many nanowires. Diameters of individual nanowires are estimated to be in the range of 10−15 nm (see Supporting Information, Figure S2). Figure 1c,d shows TEM images of the CuSe nanowire bundles showing that the nanowires are well-aligned in the bundles. A high-resolution TEM image of a single nanowire in Figure 1e shows a lattice with six-fold symmetry. A corresponding fast Fourier transform (FFT) of the lattice is shown in the inset of Figure 1e. The lattice spacing is 0.34 nm, which matches well the {100} interplanar spacing of the hexagonal CuSe crystal. An energy-dispersive X-ray (EDX) spectrum of the nanowire bundles in Figure 1f suggests that the nanowires consist only of copper and selenium with an atomic ratio of about 48:52.

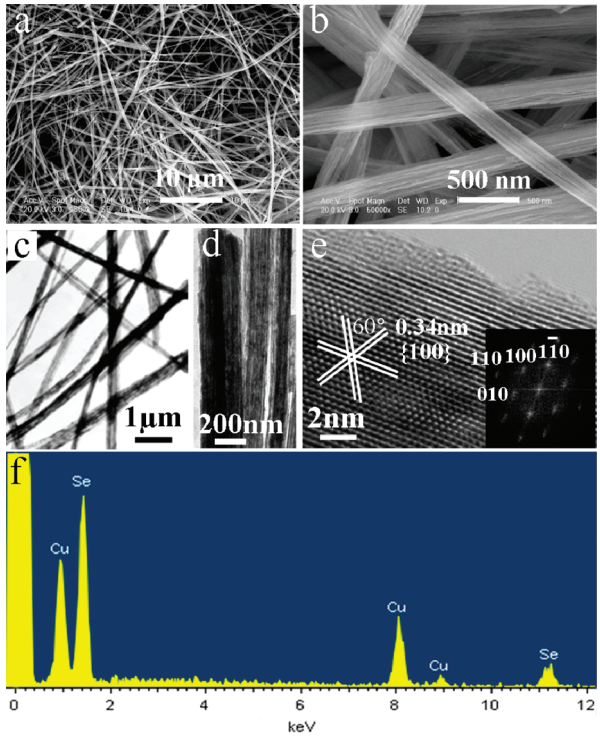

Figure 1. (a,b) SEM, (c,d) TEM, (e) high-resolution TEM images, and (f) EDX spectrum of the CuSe nanowire bundles. Inset of (e) is a fast Fourier transform (FFT) of the CuSe nanowire high-resolution TEM imaged in (e).

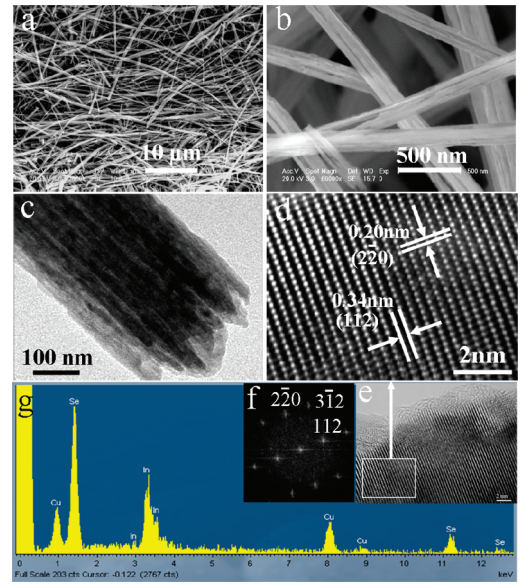

Figure 2. (a,b) SEM, (c) TEM images of $CuInSe_2$ nanowire bundles; (d,e) high-resolution TEM images of a $CuInSe_2$ nanowire; (f) a corresponding FFT of the image in (d); and (g) an EDX spectrum of the $CuInSe_2$ nanowire bundles.

By reacting the as-prepared CuSe nanowire bundles with $InCl_3$ in triethylene glycol at 200 °C, followed by immersion in a mixed solution of ethylenediamine and ethanol for several hours, $CuInSe_2$ product with morphologies similar to those of the CuSe template was obtained (Figure 2a). A high-magnification SEM image in Figure 2b and a TEM image in Figure 2c reveal that the $CuInSe_2$ bundles are made up of many well-aligned nanowires. Careful comparison with the bundles of $Cu_{2-x}Se$ and CuSe nanowires suggests that the $CuInSe_2$ nanowires have a larger diameter, which is probably due to Ostwald ripening growth during the solvothermal process (see Supporting Information, Figure S3). Figure 2d,e shows high-resolution TEM images of a $CuInSe_2$ nanowire. The lattice fringes with spacings of 0.20 and 0.34 nm match well with the interplanar spacings of the {220} and the {112} planes of chalcopyrite

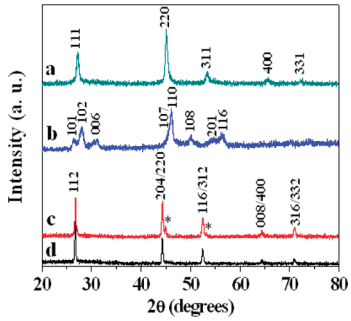

Figure 3. XRD spectra of (a) $Cu_{2-x}Se$ nanowire bundles, (b) CuSe nanowire bundles, (c) $CuInSe_2$ nanowire bundles with a trace amount of $Cu_{2-x}Se$ impurity, and (d) $CuInSe_2$ nanowire bundles.

$CuInSe_2$. An EDX spectrum (Figure 2g) of the $CuInSe_2$ nanowire bundles demonstrates that the bundles consist of copper, indium, and selenium with atomic ratios of 24:26:50.

Figure 3a shows an XRD spectrum of $Cu_{2-x}Se$ nanowire bundles. All of the diffraction peaks can be well indexed to those of cubic $Cu_{2-x}Se$ (JCPDF 06-0680). Figure 3b shows an XRD spectrum of the copper selenide sample obtained by reaction of the $Cu_{2-x}Se$ nanowire bundles with a sodium citrate solution at room temperature. The spectrum is consistent with the standard spectrum of hexagonal CuSe (JCPDF 34-0171). Figure 3c shows an XRD spectrum of the product obtained from the reaction between the as-prepared CuSe nanowire bundles and $InCl_3$ in triethylene glycol at 200 °C. All of the diffraction peaks match well to those of tetragonal $CuInSe_2$ (JCPDF 75-0107), except for the two peaks marked with an asterisk, which can be indexed to those of cubic $Cu_{2-x}Se$ (JCPDF 06-0680). This indicates the formation of the chalcopyrite $CuInSe_2$ with a small amount of $Cu_{2-x}Se$. By immersing the product in a mixed solution of ethylenediamine and ethanol for several hours, a pure phase of chalcopyrite $CuInSe_2$ was obtained, as shown in Figure 3d.

Under the solvothermal conditions, triethylene glycol plays two roles. It serves as the solvent as well as a reducing agent to reduce cupric ions (Cu^{2+}) to cuprous ions (Cu^{+}). Compared to CuSe, $Cu_{2-x}Se$ is more stable in the triethylene glycol solvent which provides a reducing environment. When $Cu_{2-x}Se$ instead of CuSe nanowire bundles are used to react with $InCl_3$ in triethylene glycol, the obtained product is a mixture of $Cu_{2-x}Se$ and In ($Cu_{2-x}Se$/In) nanowire bundles with Cu, In, and Se atomic ratios of about 61:37:2 (see Supporting Information, Figure S4). Chalcopyrite $CuInSe_2$ nanowire bundles can only be prepared by using the CuSe precursor. For the synthesis of $CuInSe_2$, CuSe is used as the precursor to react with enough indium ions. As copper ions are now in surplus, they would diffuse outward from the nanowire into the solvent during the reaction process. Therefore, it is desirable to introduce some sulfur into the system to further react with the surplus copper and indium ions.

$CuInSe_2/CuInS_2$ core/shell nanocable bundles with lengths of several tens of micrometers (see Supporting Information, Figure S5) were synthesized following the approach developed for $CuInSe_2$ nanowire bundles, but with the addition of some sublimed sulfur to the reaction system. The diameters of these nanocables are estimated to be in the range of 25−35 nm. Figure 4a−c shows high-resolution TEM images of a nanocable prepared with a S/Se molar ratio of 0.31:1, revealing a single-crystal core/polycrystalline shell structure. The diameter of the single-crystal core is estimated to be about 20 nm, while the thickness of the polycrystalline shell is in the range of 4−7 nm. In the single-crystal

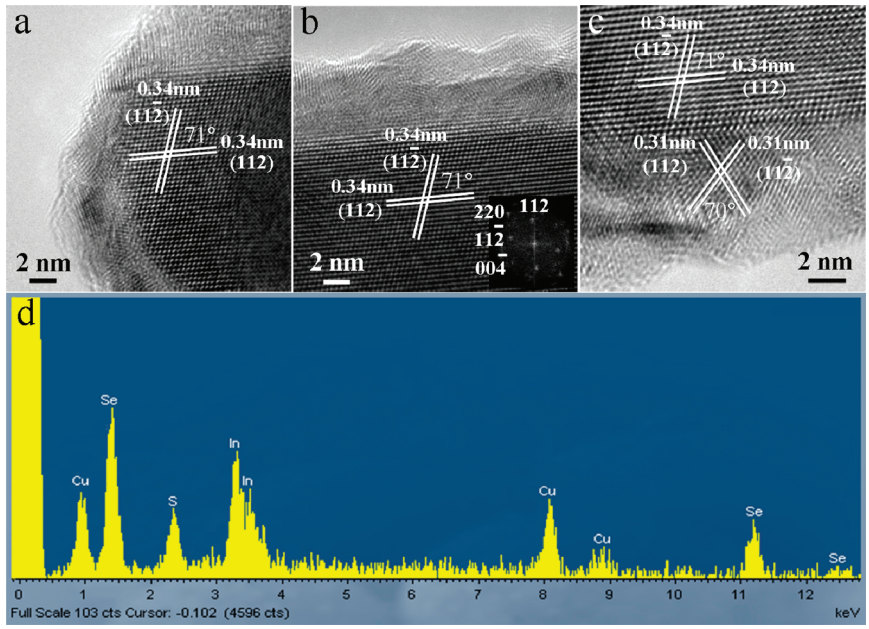

Figure 4. (a−c) High-resolution TEM images and (d) an EDX spectrum of $CuInSe_2/CuInS_2$ core/shell nanocables synthesized with a S/Se molar ratio of 0.31:1. Inset of (b): FFT of the $CuInSe_2$ core.

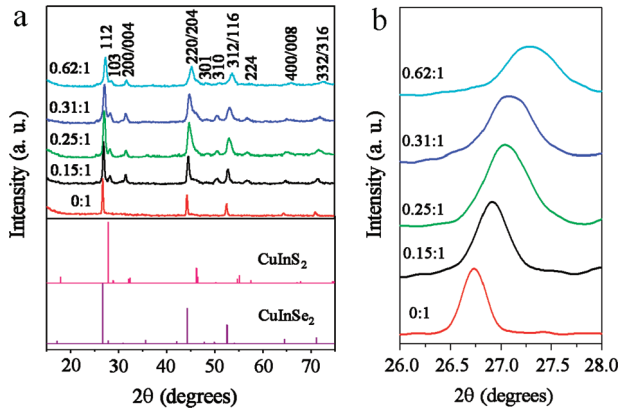

Figure 5. XRD spectra of (a) $CuInSe_2/CuInS_2$ core/shell nanocable bundles synthesized with various S/Se molar ratios, and (b) an expanded view of the (112) peaks.

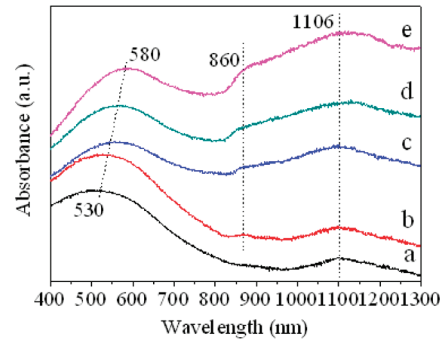

Figure 6. Room temperature absorbance spectra of the $CuInSe_2/CuInS_2$ core/shell nanocable bundles synthesized with different molar ratios of S/Se in the reactants. (a) 0:1, (b) 0.15:1, (c) 0.25:1, (d) 0.31:1, (e) 0.62:1.

core, the fringe spacing of 0.34 nm matches well to the interplanar spacing of the {112} planes of the chalcopyrite $CuInSe_2$ crystal structure. In the polycrystalline shell, as shown in Figure 4c, the fringe spacing of 0.31 nm matches well with the interplanar spacing of the {112} planes of chalcopyrite $CuInS_2$. An EDX spectrum of the nanocables shown in Figure 4d confirms the presence of copper, indium, selenium, and sulfur. It was observed that the thickness of the polycrystalline $CuInS_2$ shell in the nanocables increases with increasing S/Se molar ratio in the reactants (see Supporting Information, Figures S6 and S7).

The $CuInSe_2/CuInS_2$ core/shell nanocables are considered to form *via* a solid−liquid reaction mechanism, which is controlled by the outward diffusion of copper ions. In the high boiling point triethylene glycol solvent, the added sulfur powders would first dissolve in the solvent during the heating process. While the CuSe nanowires react with the inward diffused indium ions to convert into $CuInSe_2$, surplus copper ions diffuse outward to react with the dissolved sulfur atoms/anions to form CuS and further evolve into $CuInS_2$ with the reaction of indium ions on the surface of the nanowires, resulting in the formation of the $CuInSe_2/CuInS_2$ core/shell nanocables. Due to the relatively large size of sulfur atoms/ions, their inward diffusion is negligible.[31] The reaction of sulfur, copper ions, and indiums ions to form tetragonal $CuInS_2$ is further confirmed by the reaction of S powder, $Cu(NO_3)_2$, and $InCl_3$ in triethylene glycol, as shown in Figure S8 (Supporting Information). In our case, the added sulfur is considered to play an important role in the formation of the $CuInSe_2/CuInS_2$ core/shell nanocable bundles in at least three aspects: (i) sulfur enhances the driving force for outward diffusion of copper ions; (ii) it avoids the formation of binary impurity of $Cu_{2-x}Se$; (iii) it provides the sulfur source for the formation of the $CuInS_2$ shell.

Figure 5a shows XRD data of the as-prepared $CuInSe_2/CuInS_2$ core/shell nanocable bundles synthesized with different S/Se molar ratios. These spectra closely resemble those of the $CuInSe_2$ core (0:1), but with the appearance of several minor peaks, which distinguishing the chalcopyrite phase from the sphalerite phase. Figure 5b shows an expanded view of the (112) diffraction peaks in Figure 5a. With increasing S/Se contents, the diffraction peaks broaden and shift to higher angles. These changes are attributed to the stacking faults and smaller crystal domain size in/of the polycrystalline $CuInS_2$ shell. This observation is consistent with the HRTEM results (Figure 4 and Figure S6). The progressive shifts in the diffraction peak positions are consistent with the composition changes in the core/shell nanocable (Figure 4 and Figure S7). On the other hand, broadening of the diffraction peaks is attributed to the growth of a polycrystalline $CuInS_2$ shell on the surface of the single-crystal $CuInSe_2$ core.

Vis−NIR spectrophotometry was used to characterize optical absorption properties of the obtained $CuInSe_2/CuInS_2$ core/shell nanowire bundles synthesized with different S/Se molar ratios in the source materials. For the measurements, these products were dispersed in absolute ethanol by ultrasonication. Spectrum a (Figure 6) of the $CuInSe_2$ nanowire bundles exhibits a weak broad absorption peak centered at ~1106 nm (~1.12 eV), which corresponds to the expected band gap energy of ~1.04 eV of $CuInSe_2$. Enhanced optical absorption of the $CuInSe_2/CuInS_2$ core/shell nanocable bundles in the range of 800−1300 nm is demonstrated as shown in spectra b−e. These spectra show the emergence of a shoulder at ~860 nm (~1.44 eV), indicating the formation of the $CuInS_2$ shell (E_g = 1.53 eV). The upper valence band of $CuInSe_2$ and $CuInS_2$ consists of nonlocalized and localized states. The nanolocalized states are due to p−d hybridization, while the localized ones are due to d electron states of copper. Absorption peaks around 530−580 nm were also observed, which are considered to originate from the nonbonding copper d localized states.[32] The absorption energies are attributed to the non-ground-state absorption energy of $CuInSe_2$ and $CuInS_2$. Clearly, the $CuInSe_2/CuInS_2$ core/shell structures show broad optical absorption over the vis−NIR region, which may be beneficial for their photovoltaic applications.

CONCLUSIONS

CuSe was demonstrated to be a good precursor for fabricating chalcopyrite $CuInSe_2$-based nanostructures with inherited morphologies in large scale. CuSe nanowire bundles with lengths up to hundreds of micrometers have been synthesized by reacting $Cu_{2-x}Se$ nanowire bundles with sodium citrate solution. Chalcopyrite $CuInSe_2$ nanowire bundles have been synthesized in large scale by using these as-prepared CuSe nanowire bundles as self-sacrificial templates to react with $InCl_3$ *via* a solvothermal method, in which the solvent of triethylene glycol also serves as a reducing reagent. The synthesis of chalcopyrite $CuInSe_2/CuInS_2$ core/shell nanowire bundles with various S/Se molar ratios has been demonstrated, in which the fast outward diffusion of copper ions is responsible for the formation of $CuInS_2$ shell. Broad optical absorption over the vis−NIR region of $CuInSe_2/CuInS_2$ core/shell nanowire bundles was demonstrated.

EXPERIMENTAL SECTION

Synthesis of $Cu_{2-x}Se$ Nanowire Bundles. Synthesis of $Cu_{2-x}Se$ nanowire bundles has been described elsewhere.[28] In a typical synthesis, 0.15 g of Se powder, 4.5 g of NaOH, and 20 mL of distilled water were put in a 100 mL beaker with heating and stirring to make an alkaline selenium aqueous solution. Then 1.5 mL of $Cu(NO_3)_2$ aqueous solution (0.50 M) was then added. $Cu_{2-x}Se$ nanowire bundles were obtained after drying the solution in a fan-forced oven at 140 °C. The nanowire bundles were collected and washed with hot distilled water and ethanol several times and then dried under vacuum.

Synthesis of CuSe Nanowire Bundles. CuSe nanowire bundles were prepared by immersing $Cu_{2-x}Se$ nanowire bundles in an aqueous sodium citrate solution (0.1 M) with gentle stirring at room temperature for 18−30 h. The product was separated by centrifugation, washed with distilled water and absolute ethanol, and then dried under vacuum for 12 h.

Synthesis of $CuInSe_2$ Nanowire Bundles. $InCl_3$ (0.01 g) was first dissolved in 30 mL of triethylene glycol in a Teflon-lined stainless steel autoclave; 0.045 g of CuSe nanowire bundles was then dispersed into the solution by stirring and ultrasonication. The autoclave was then sealed and maintained at 180−200 °C for 40 h. After cooling to room temperature naturally, reaction product was collected and washed with absolute ethanol several times. The product was then immersed in a 1:1 mixture of anhydrous ethylenediamine and absolute ethanol under gentle stirring for several hours. Precipitates were finally separated by centrifugation, washed with absolute ethanol, and then dried under vacuum for 12 h.

Synthesis of $CuInSe_2/CuInS_2$ Core/Shell Nanowire Bundles. $InCl_3$ (0.01 g), CuSe nanowire bundles (0.045 g), and various amounts of sublimed sulfur were dispersed or dissolved in 30 mL of triethylene glycol by stirring and ultrasonication in a Teflon-lined stainless steel autoclave. The autoclave was then sealed and maintained at 180−200 °C for 40 h. After cooling to room temperature naturally, the reaction product was collected and washed with absolute ethanol several times and then dried under vacuum for 12 h.

Characterization of Samples. As-prepared samples were characterized *via* X-ray diffraction (XRD) in a Philips X'Pert diffractometer with a Cu Kα radiation source. Scanning electron microscopy (SEM) was carried out with a Philips XL30 FEG SEM. Transmission electron microscopic (TEM) images and high-resolution TEM images were taken with a Philips CM 20 FEG TEM and a Philips CM 200 FEG TEM, respectively, operated at 200 kV. Absorption spectra were recorded with a PE Lambda 19 spectrophotometer.

Acknowledgment. This project has been financially supported by Research Grants of HKSAR (No. 7002271), and the National Natural Science Foundation of China (NSFC Grants 20871038, 20876031).

Supporting Information Available: SEM images of the $Cu_{2-x}Se$ nanowire bundles, high-resolution TEM image and high-magnification SEM image of CuSe nanowires, high-resolution TEM image and high-magnification SEM image of $CuInSe_2$ nanowires, XRD spectrum and EDX spectrum of $Cu_{2-x}Se$/In nanowire bundles, SEM and TEM images of $CuInSe_2/CuInS_2$ core/shell nanocable bundles with a S/Se molar ratio of 0.31:1, high-resolution TEM images and EDX spectra of $CuInSe_2/CuInS_2$ core/shell nanocables with various S/Se molar ratios. XRD spectra of the products prepared with $Cu(NO_3)_2$, $InCl_3$, and S in triethylene glycol. This material is available free of charge *via* the Internet at http://pubs.acs.org.

REFERENCES AND NOTES

1. Hsu, Y.-J.; Hung, C.-M.; Lin, Y.-F.; Liaw, B.-J.; Lobana, T. S.; Lu, S.-Y.; Liu, C. W. $[Cu_4\{Se_2P(O^iPr)_2\}_4]$: A Novel Precursor Enabling Preparation of Nonstoichiometric Copper Selenide ($Cu_{2-x}Se$) Nanowires. *Chem. Mater.* **2006**, *18*, 3323–3329.
2. Yu, X. L.; Cao, C. B.; Zhu, H. S.; Li, Q. S.; Liu, C. L.; Gong, Q. H. Nanometer-Sized Copper Sulfide Hollow Spheres with Strong Optical-Limiting Properties. *Adv. Funct. Mater.* **2007**, *17*, 1397–1401.
3. Tang, J.; Hinds, S.; Kelley, S. O.; Sargent, E. H. Synthesis of Colloidal $CuGaSe_2$, $CuInSe_2$, and $Cu(InGa)Se_2$ Nanoparticles. *Chem. Mater.* **2008**, *20*, 6906–6910.
4. Dhere, N. G. Toward GW/Year of CIGS Production within the Next Decade. *Sol. Energy Mater. Sol. Cells* **2007**, *91*, 1376–1382.
5. Xie, R. G.; Rutherford, M.; Peng, X. G. Formation of High-Quality I−III−VI Semiconductor Nanocrystals by Tuning Relative Reactivity of Cationic Precursors. *J. Am. Chem. Soc.* **2009**, *131*, 5691–5697.
6. Allen, P. M.; Bawendi, M. G. Ternary I−III−VI Quantum Dots Luminescent in the Red to Near-Infrared. *J. Am. Chem. Soc.* **2008**, *130*, 9240–9241.
7. Beck, M. E.; Swartzlander-Guest, A.; Matson, R.; Keane, J.; Noufi, R. CuIn(Ga)Se_2-Based Devices *via* a Novel Absorber Formation Process. *Sol. Energy Mater. Sol. Cells* **2000**, *64*, 135–165.
8. Guo, Q. J.; Ford, G. M.; Hillhouse, H. W.; Agrawal, R. Sulfide Nanocrystal Inks for Dense $Cu(In_{1-x}Ga_x)(S_{1-y}Se_y)_2$ Absorber Films and Their Photovoltaic Performance. *Nano Lett.* **2009**, *9*, 3060–3065.
9. Guillemoles, J.-F.; Kronik, L.; Cahen, D.; Rau, U.; Jasenek, A.; Schock, H.-W. Stability Issues of Cu(In,Ga)Se_2-Based Solar Solar Cells. *J. Phys. Chem. B* **2000**, *104*, 4849–4862.
10. Ward, J. S.; Ramanathan, K.; Hasoon, F. S.; Coutts, T. J.; Keane, J.; Contreras, M. A.; Moriarty, T.; Noufi, R. A 21.5% Efficient Cu(In,Ga)Se_2 Thin-Film Concentrator Solar Cell. *Prog. Photovoltaics* **2002**, *10*, 41–46.
11. Rockett, A.; Birkmire, R. W. $CuInSe_2$ for Photovoltaic Application. *J. Appl. Phys.* **1991**, *70*, R81–R97.
12. Yüksel, Ö. F.; Başol, B. M.; Şafak, H.; Karabiyik, H. Optical Characterisation of $CuInSe_2$ Thin Films Prepared by Two-Stage Process. *Appl. Phys. A: Mater. Sci. Process.* **2001**, *73*, 387–389.
13. Castro, S. L.; Bailey, S. G.; Raffaelle, R. P.; Banger, K. K.; Hepp, A. F. Nanocrystalline Chalcopyrite Materials ($CuInS_2$ and $CuInSe_2$) *via* Low-Temperature Pyrolysis of Molecular Single-Source Precursors. *Chem. Mater.* **2003**, *15*, 3142.

14. Adurodija, F. O.; Song, J.; Kim, S. D.; Kwon, S. H.; Kim, S. K.; Yoon, K. H.; Ahn, B. T. Growth of $CuInSe_2$ Thin Films by High Vapour Se Treatment of Co-Sputtered Cu−In Alloy in a Graphite Container. *Thin Solid Films* **1999**, *338*, 13–19.
15. Zhang, L.; Jiang, F. D.; Feng, J. Y. Formation of $CuInSe_2$ and $Cu(In,Ga)Se_2$ Films by Electrodeposition and Vacuum Annealing Treatment. *Sol. Energy Mater. Sol. Cells* **2003**, *80*, 483–490.
16. Igasaki, Y.; Maeda, M.; Harada, M.; Fujiwara, T. Preparation of $CuInSe_2$ Film by Hot-Wall Evaporation Technique. *J. Cryst. Growth* **1996**, *167*, 769–772.
17. Artaud, M. C.; Ouchen, F.; Martin, L.; Duchemin, S. CuInSe Thin Films Grown by MOCVD: Characterization, First Devices. *Thin Solid Films* **1998**, *324*, 115–123.
18. Vassilev, G. P.; Docheva, P.; Nancheva, N.; Arnaudov, B.; Dermendjiev, I. Technology and Properties of Magnetron Sputtered $CuInSe_2$ Layers. *Mater. Chem. Phys.* **2003**, *82*, 905–910.
19. Nie, H. B.; Wang, Y. L.; Ni, P. R.; Guo, S. J. Preparation of $CuInSe_2$ Thin Films by Paste Coating. *Rare Metals* **2008**, *27*, 591–597.
20. Li, B.; Xie, Y.; Huang, J. X.; Qian, Y. T. Synthesis by a Solvothermal Route and Characterization of $CuInSe_2$ Nanowhiskers and Nanoparticles. *Adv. Mater.* **1999**, *11*, 1456–1459.
21. Jiang, Y.; Wu, Y.; Mo, X.; Yu, W. C.; Xie, Y.; Qian, Y. T. Elemental Solvothermal Reaction to Produce Ternary Semiconductor $CuInE_2$ (E = S, Se) Nanorods. *Inorg. Chem.* **2000**, *39*, 2964–2965.
22. Yang, Y.-H.; Chen, Y.-T. Solvothermal Preparation and Spectroscopic Characterization of Copper Indium Diselenide Nanorods. *J. Phys. Chem. B* **2006**, *110*, 17370–17374.
23. Guo, Q. J.; Kim, S. J.; Kar, M.; Shafarman, W. N.; Birkmire, R. W.; Stach, E. A.; Agrawal, R.; Hillhouse, H. W. Development of $CuInSe_2$ Nanocrystal and Nanoring Inks for Low-Cost Solar Cells. *Nano Lett.* **2008**, *8*, 2982–2987.
24. Koo, B.; Patel, R. N.; Korgel, B. A. Synthesis of $CuInSe_2$ Nanocrystals with Trigonal Pyramidal Shape. *J. Am. Chem. Soc.* **2009**, *131*, 3134–3135.
25. Panthani, M. G.; Akhavan, V.; Goodfellow, B.; Schmidtke, J. P.; Dunn, L.; Dodabalapur, A.; Barbara, P. F.; Korgel, B. A. Synthesis of $CuInS_2$, $CuInSe_2$, and $Cu(In_xGa_{1-x})Se_2$ (CIGS) Nanocrystal "Inks" for Printable Photovoltaics. *J. Am. Chem. Soc.* **2008**, *130*, 16770–16777.
26. Peng, H. L.; Schoen, D. T.; Meister, S.; Zhang, X. F.; Cui, Y. Synthesis and Phase Transformation of In_2Se_3 and $CuInSe_2$ Nanowires. *J. Am. Chem. Soc.* **2007**, *129*, 34–35.
27. Schoen, D. T.; Peng, H. L.; Cui, Y. Anisotropy of Chemical Transformation from In_2Se_3 to $CuInSe_2$ Nanowires through Solid State Reaction. *J. Am. Chem. Soc.* **2009**, *131*, 7973–7975.
28. Xu, J.; Zhang, W. X.; Yang, Z. H.; Ding, S. X.; Zeng, C. Y.; Chen, L. L.; Wang, Q.; Yang, S. H. Large-Scale Synthesis of Long Crystalline $Cu_{2-x}Se$ Nanowire Bundles by Water-Evaporation-Induced Self-Assembly and Their Application in Gas Sensing. *Adv. Funct. Mater.* **2009**, *19*, 1759–1766.
29. Parkinson, J. A.; Sun, H. Z.; Sadler, P. J. New Approach to the Solution Chemistry of Bismuth Citrate Antiulcer Complexes. *Chem. Commun.* **1998**, 881–882.
30. Dean, J. A. *Lange's Hand Book of Chemistry*; 15th ed.; McGraw-Hill, Inc.: New York, 1999; section 8, p 90.
31. Cao, H. L.; Qian, X. F.; Wang, C.; Ma, X. D.; Yin, J.; Zhu, Z. K. High Symmetric 18-Facet Polyhedron Nanocrystals of Cu_7S_4 with a Hollow Nanocage. *J. Am. Chem. Soc.* **2005**, *127*, 16024–16025.
32. Xiao, J. P.; Xie, Y.; Xiong, Y. J.; Tang, R.; Qian, Y. T. A Mild Solvothermal Route to Chalcopyrite Quaternary Semiconductor $CuIn(Se_xS_{1-x})_2$ Nanocrystallites. *J. Mater. Chem.* **2001**, *11*, 1417–1420.